한국전산구조공학회
2002년도 가을 학술발표회 논문집

# 부분 분포하중이 재하된 직4각형 평판의 임계하중

# Elastic Critical Loads of Rectangular Plates Under Patch Loads

이수곤[*] 김순철[**] 송용욱[***] 송상용[***]
Lee, Soo-Gon Kim, Soon-Chul Song, Yong-Yuk Song, Sang-Yong

## 국문초록

주변이 Kinney의 정의에 따른 부분 고정도를 가지고 지지된 직4각형 평판이 부분 분포하중을 받고 있을 때의 안정해석을 유한 요소법으로 수행하였다. 수치해석에서 고려한 변수는 평판의 변장비 ( $=\lambda$)와 부분 분포하중 작용폭 ( $=\gamma$) 및 부분 고정도 ( $=f$ ) 값이다. 여기서 특히 $f=0.0$ 은 주변이 단순지지를 표시하고 $f=1.0$은 고정지지를 뜻하는데 수치해석에서는 $f=0.0, 0.2, \cdots, 1.0$으로 변화시켰다. 유한 요소법으로 산정한 판의 좌굴계수 변화는 각각의 변장비에 대하여 나머지 두 개의 매개변수를 변량으로 하는 대수 함수식으로 표시하였다. 제안한 대수식으로 추정한 임계하중치와 유한 요소법으로 산정한 임계하중치 간의 상관계수는 모든 변장비에 대하여 거의 단위치 ( $\rho\approx 1.0$)에 가까웁다. 따라서 제안한 대수 함수식은 구조 설계자들의 판 설계 및 안정 검토시에 유익한 자료로 이용될 수 있다.

## I. Introduction

The elastic critical loads of rectangular plates can be the prime factor to be considered when one encounters the design or stability check of silos, bins, web parts of wide flange beams and building shear walls. The stability of rectangular plates has been widely studied over the last century by many researchers. However, when the plates with partially fixed edges are subjected to partially distributed (or patch) loads, the information for the design aids is scarce.

In this study, the stability analysis of the plate under different loading conditions is carried out by the finite element method. The parameters considered in the analysis are aspect ratio ( $=\lambda$) and patch load width factor ( $=\gamma$). The boundary conditions for the plate edges are expressed in terms of Kinney's fixity factor. According to Kinney's fixity factor, fixity factor is zero ( $f=0.0$) when the plate edge is simply supported and unity ( $f=1.0$) when the edge is completely fixed.

* 전남대학교 건축학과 교수
** 동신대학교 건축학과 교수
*** 전남대학교 석사과정

For easy determination of critical load of the plate or for fast check of plate stability, the changes of critical load coefficient is expressed by an algebraic equation of analysis parameters for each boundary condition. The critical load coefficients estimated by the proposed equation coincide fairly well with those determined by the finite element analysis. The differences of critical load coefficients of two different loading conditions can be a measure to determine the difference of plate strength, for which they are also represented by algebraic equations of analysis parameters.

## 2. Problem Definition

Fig. 1 shows the two in-plane loading conditions and they are designated as LC1 and LC2. In the

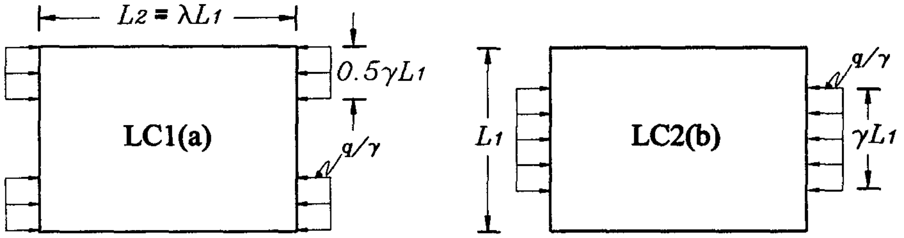


Fig. 1 Loading conditions and symbols

study, the patch load width factor, $\gamma$ is made to change from zero ( $\gamma=0.0$, concentrated load) to unity ( $\gamma=1.0$, uniform load along the full edge). Also shown in the picture is the aspect ratio, $\lambda$, which is to be varied from unity ( $\lambda=1.0$, square plate) to 3.0 ( $\lambda=3.0$) with subinterval 0.2.

When the plate edges are supported by edge beams, the rotations are partially restrained. To quantity the restraint effect at the plate edges, boundary conditions shown in Fig. 2 are also expressed in terms of Kinney's fixity factor $f$. The numerical values of fixity factor are already given in the Introduction.

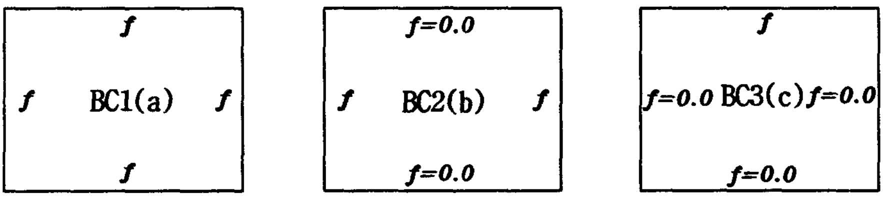


Fig. 2 Boundary conditions for the plate

As one would guess, the conventional method, for example, neutral equilibrium method or Rayleigh-Ritz method is difficult to apply to the stability analysis of present plates. The application of Rayleigh-Ritz method to the plate under concentrated loads at the plate edge centers requires complicated calculations only to obtain approximate results.

## 3. Element Stiffness Matrices

Fig. 3 shows a rectangular element having 3 d.o.fs at each node, whose displacement function can be used in the derivation of the element stiffness matrices. In the picture, the $q_i$ in parenthesis denotes

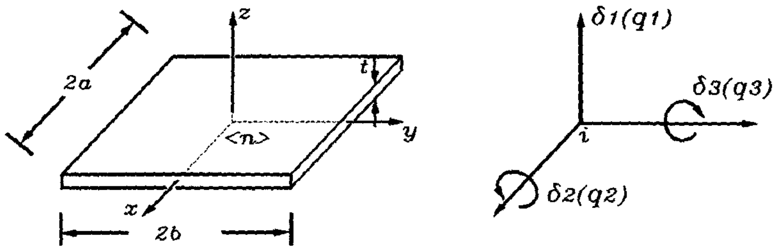


Fig. 3 Displacement and force compomemts of a rectangular plate

the generalized force component corresponding to generalized displacement component, $\delta_i$.

The element displacement function is usually assumed to be the following polynomial of $x$, $y$.

$$w = A_1 + A_2x + A_3y + A_4x^2 + A_5xy + A_6y^2 + A_7x^3 + A_8x^2y + A_9xy^2 + A_{10}y^3 + A_{11}x^3y + A_{12}xy^3 \quad (1)$$

The coefficients, $A_1, A_2, \cdots, A_{12}$ can be expressed by the nodal displacement components, $\delta_i$s, which lead to the following

$$w = [f_1, f_2, \cdots, f_{12}]\begin{Bmatrix} \delta_1 \\ \delta_2 \\ \vdots \\ \delta_{12} \end{Bmatrix} = [f]\{\delta\} \quad (2)$$

where $[f]$ denotes shape function set, whose components are given by ( $e = 1/8$, $\xi = x/a$, $\eta = y/b$)

$$\begin{aligned} &f_1 = e(1-\xi)(1-\eta)(2-\xi^2-\eta^2-\xi-\eta), && f_2 = e(1-\xi)(1-\eta)(1-\xi^2)a \\ &f_3 = e(1-\xi)(1-\eta)(1-\eta^2)b, && f_4 = e(1-\xi)(1+\eta)(2-\xi^2-\eta^2-\xi+\eta) \\ &f_5 = e(1-\xi)(1+\eta)(1-\xi^2)a, && f_6 = -e(1-\xi)(1+\eta)(1-\eta^2)b \\ &f_7 = e(1+\xi)(1+\eta)(2-\xi^2-\eta^2+\xi+\eta), && f_8 = -e(1+\xi)(1+\eta)(1-\xi^2)a \\ &f_9 = -e(1+\xi)(1+\eta)(1-\eta^2)b, && f_{10} = e(1+\xi)(1-\eta)(2-\xi^2-\eta^2+\xi-\eta) \\ &f_{11} = -e(1+\xi)(1-\eta)(1-\xi^2)a, && f_{12} = e(1+\xi)(1-\eta)(1-\eta^2)b \end{aligned} \quad (3)$$

When deriving element stiffness matrices, it is convenient to start with the flexural strain energy of the plate element, $U$

$$U = \frac{1}{2}\int_{-b}^{b}\int_{-a}^{a}\{M\}^T\{\Phi\}dxdy \quad (4)$$

in which

$$\{M\} = \begin{Bmatrix} M_x \\ M_y \\ M_{xy} \end{Bmatrix} = D\begin{vmatrix} 1 & v & 0 \\ v & 1 & 0 \\ 0 & 0 & 0.5(1-v) \end{vmatrix}\begin{Bmatrix} \frac{\partial^2 w}{\partial x^2} \\ \frac{\partial^2 w}{\partial y^2} \\ 2\frac{\partial^2 w}{\partial x \partial y} \end{Bmatrix} = [D]\{\Phi\} \quad (5)$$

when Eq. (2) is used, curvature vector, $\{\Phi\}$ is given by the derivatives of the shape functions ;

$$\{\Phi\}=\begin{Bmatrix} \dfrac{\partial^2 f}{\partial x^2} \\ \dfrac{\partial^2 f}{\partial y^2} \\ 2\dfrac{\partial^2 f}{\partial x \partial y} \end{Bmatrix}\{\delta\}=[C]\{\delta\} \tag{6}$$

Substitution of Eq. (6) and (5) into Eq. (4), leads to

$$U=\frac{1}{2}\{\delta\}^T\left(\int_{-b}^{b}\int_{-a}^{a}[C]^T[D][C]dxdy\right)\{\delta\} \tag{7}$$

The external work for the element is given by

$$\begin{aligned} W&=\frac{1}{2}\{q\}^T\{\delta\}+\frac{1}{2}\int_{-b}^{b}\int_{-a}^{a}[\alpha]^T[N][\alpha]dxdy \\ &=\frac{1}{2}\{\delta\}^T\left([k]+\int_{-b}^{b}\int_{-a}^{a}[B]^T[N][B]dxdy\right)\{\delta\} \end{aligned} \tag{8}$$

in which rotation vector, $\{\alpha\}$

$$\{\alpha\}=\begin{Bmatrix} \dfrac{\partial w}{\partial x} \\ \dfrac{\partial w}{\partial y} \end{Bmatrix}=\begin{Bmatrix} \dfrac{\partial f}{\partial x} \\ \dfrac{\partial f}{\partial y} \end{Bmatrix}\{\delta\}=[B]\{\delta\} \tag{9}$$

and $[N]$, the in-plane force set

$$[N]=\begin{vmatrix} N_x & N_{xy} \\ N_{yx} & N_y \end{vmatrix} \tag{10}$$

The plane stress analysis of the whole plate under the loading conditions of Fig. (1) leads the determination of Eq. (10) for each element.

Equating the strain energy, $U$ to the external work, $W$ and rearranging terms, one obtains

$$[k]=[k_b]-[k_g]=\int_{-b}^{b}\int_{-a}^{a}[C]^T[D][C]dxdy-\int_{-b}^{b}\int_{-a}^{a}[B]^T[N][B]dxdy \tag{11}$$

In the above, $[k_b]$ and $[k_g]$ denote flexural and geometric stiffness matrix, respectively. The actual integrations of Eq. (11) involve complicated calculations and so only the final results are listed in Table (1) and (2).

Table (1). Flexural stiffness matrix

$$[k_b]=\frac{D}{60ab}\begin{bmatrix}
60p+60p^{-1}-42-12\mu & & & & & & & & & & & \\
b(60p+6+24\mu) & b^2(80p+16-16\mu)\times F & & & & & & & & & & \\
a(60p^{-1}+6+24\mu) & 60\mu ab & a^2(80p^{-1}+16-16\mu)\times F & & & & & & & & & \\
30p-60p^{-1}-42+12\mu & b(30p-6-24\mu) & a(-60p^{-1}-6+6\mu) & k_{1,1} & & & & & & & & \\
k_{4,2} & b^2(40p-16+16\mu) & 0 & k_{2,1} & k_{2,2}\times F & & & & & & & \\
-k_{4,3} & -k_{5,3} & a^2(40p^{-1}-4+4\mu) & -k_{3,1} & -k_{3,2} & k_{3,3}\times F & & & & & & \\
30p-30p^{-1}+42-12\mu & b(-30p+6-6\mu) & a(-30p^{-1}+6-6\mu) & k_{10,1} & k_{10,2} & -k_{10,3} & k_{1,1} & & & & & \\
-k_{7,2} & b^2(20p+4-4\mu) & 0 & k_{11,1} & k_{11,2} & -k_{11,3} & -k_{2,1} & k_{2,2}\times F & & & & \\
-k_{7,3} & k_{8,3} & a^2(20p^{-1}+4-4\mu) & -k_{12,1} & -k_{12,2} & k_{12,3} & -k_{3,1} & k_{3,2} & k_{3,3}\times F & & & \\
-60p+30p^{-1}-42+12\mu & b(-60p-6+6\mu) & a(-30p^{-1}-6+24\mu) & k_{7,1} & k_{7,2} & -k_{7,3} & k_{4,1} & -k_{4,2} & -k_{4,3} & k_{1,1} & & \\
-k_{10,2} & b^2(40p-4+4\mu) & 0 & k_{8,1} & k_{8,2} & -k_{8,3} & -k_{5,1} & k_{5,2} & k_{5,3} & -k_{2,1} & k_{2,2}\times F & \\
-k_{10,3} & -k_{11,3} & a^2(40p^{-1}-16+16\mu) & -k_{9,1} & -k_{9,2} & k_{9,3} & -k_{6,1} & k_{6,2} & k_{6,3} & k_{3,1} & -k_{3,2} & k_{3,3}\times F
\end{bmatrix}$$

symm

* $p=(a/b)^2$
* $F=1/(1-f)$

Table (2). Geometric stiffness matrix

$$[k_n]_g = -\frac{qtb}{630a}\begin{bmatrix} 276 & & & & & & & & & & & \\ 66b & 24b^2 & & & & & & & & & & \text{symm.} \\ 42a & 0 & 112a^2 & & & & & & & & & \\ -276 & -66b & -42a & k_{1,1} & & & & & & & & \\ -66b & -24b^2 & 0 & k_{2,1} & k_{2,2} & & & & & & & \\ 42a & 0 & -28a^2 & -k_{3,1} & -k_{3,2} & k_{3,3} & & & & & & \\ -102 & -39b & -21a & k_{10,1} & k_{10,2} & -k_{10,3} & k_{1,1} & & & & & \\ 39b & 18b^2 & 0 & k_{11,1} & k_{11,2} & -k_{11,3} & -k_{2,1} & k_{2,2} & & & & \\ 21a & 0 & -14a^2 & -k_{12,1} & -k_{12,2} & k_{12,3} & -k_{3,1} & k_{3,2} & k_{3,3} & & & \\ 102 & 39b & 21a & k_{7,1} & k_{7,2} & -k_{7,3} & k_{4,1} & -k_{4,2} & -k_{4,3} & k_{1,1} & & \\ -39b & -18b^2 & 0 & k_{8,1} & k_{8,2} & -k_{8,3} & -k_{5,1} & k_{5,2} & k_{5,3} & -k_{2,1} & k_{2,2} & \\ 21a & 0 & 56a^2 & -k_{9,1} & -k_{9,2} & k_{9,3} & -k_{6,1} & k_{6,2} & k_{6,3} & k_{3,1} & -k_{3,2} & k_{3,3} \end{bmatrix}$$

The terms $F$s in Table (1) are introduced to include the edge restraint effect in terms of fixity factor, $f$.

## 4. Critical Load Determination

Subdivision of the plate into elements, determination of element matrices for each element, assembly of matrices and finally the application of boundary conditions to the assembled matrices lead to the following form of matrix equation

$$([K_b] - q[K_g])\{\triangle\} = \{Q\}, \quad \{Q\} = \{0\} \tag{12}$$

in which $\{\triangle\}$ denotes nodal displacement vector for the plate.

The determination of the least eigenvalue by computer-aided iteration technique needs the following transformation first.

$$\left([K_b]^{-1}[K_g] - \frac{1}{q}[I]\right)\{\triangle\} = \{0\} \tag{13}$$

in which $[I]$ denotes identity (unit) matrix. To examine the in-house developed finite element program, the square plate shown in Fig. 4 is subdivided into elements as indicated in the picture and critical loads are determined by repeating precedures of Eq. (12) and (13).

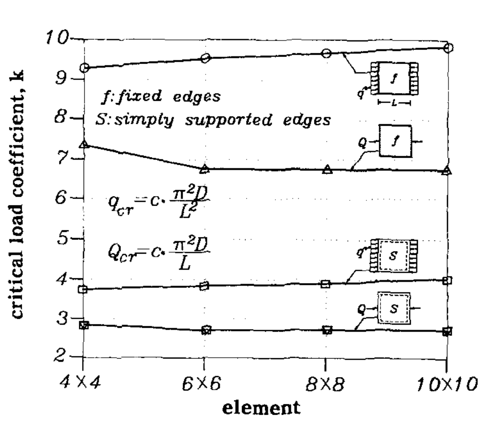


Fig. 4 Critical load convergence

As one would see in the picture, the critical load coefficients, $C$s converge to certain values with increasing subdivisions. In the cases of full edge load, $q$, the developed program yields $C = 3.96$ (exact, 4.0) for simply supported edges and $C = 9.87$ (exact, 10.07) for fixed edges. In the cases of concentrated force, $Q$ the proposed method gives $C = 2.63$ (Narayanan, 2.68) for simply supported edges. For the fixed edges, developed program yields $C = 6.72$ (Yamaki, 7.30). From these comparisons, one can observe insignificant errors in all cases except the case of fixed plate under concentrated edge load.

In the present study, critical load coefficients ( $= C_{fem}$s) are determined by subdividing plate into $10\times10$ (when $\lambda=1.0$), $10\times12$ (when $\lambda=1.2$), $\cdots$, elements. Because of space limit, some of the results only are listed in Table (3).

Table (3). Critical load coefficients

<Fig. 1(a), Fig. 2(a)>

| $\lambda$= 1.0 | $\gamma$= 0.0 | | $\gamma$ = 0.2 | | $\gamma$ = 0.4 | | $\gamma$ = 0.6 | | $\gamma$ = 0.8 | | $\gamma$ = 1.0 | |
|---|---|---|---|---|---|---|---|---|---|---|---|---|
| $f$ | $C_{fem}$ | $C_{est}$ | $C_{fem}$ | $C_{est}$ | $C_{fem}$ | $C_{est}$ | $C_{fem}$ | $C_{est}$ | $C_{fem}$ | $C_{est}$ | $C_{fem}$ | $C_{est}$ |
| **0.0** | 6.0912 | 6.2918 | 6.0307 | 6.0595 | 5.6738 | 5.7097 | 5.0493 | 5.2425 | 4.4207 | 4.6578 | 3.9577 | 3.9557 |
| **0.2** | 8.6351 | 8.5242 | 8.5711 | 8.2861 | 8.1962 | 7.9056 | 7.5048 | 7.3826 | 6.7350 | 6.7172 | 6.1233 | 5.9093 |
| **0.4** | 10.3179 | 10.3298 | 10.2432 | 10.0791 | 9.8289 | 9.6665 | 9.1060 | 9.0921 | 8.2947 | 8.3558 | 7.6256 | 7.4577 |
| **0.6** | 11.5181 | 11.7086 | 11.4359 | 11.4383 | 10.9712 | 10.9924 | 9.3372 | 9.5738 | 9.3372 | 9.5738 | 8.6193 | 8.6700 |
| **0.8** | 12.4393 | 12.6606 | 12.3527 | 12.3639 | 11.8434 | 11.8834 | 11.0065 | 11.2191 | 10.0931 | 10.3710 | 9.3243 | 9.3391 |
| **1.0** | 13.1855 | 13.1858 | 13.0948 | 12.8558 | 12.5503 | 12.3394 | 11.6574 | 11.6367 | 10.6870 | 10.7475 | 9.8695 | 9.6720 |

<Fig. 1(b), Fig. 2(a)>

| $\lambda$= 1.0 | $\gamma$= 0.0 | | $\gamma$ = 0.2 | | $\gamma$ = 0.4 | | $\gamma$ = 0.6 | | $\gamma$ = 0.8 | | $\gamma$ = 1.0 | |
|---|---|---|---|---|---|---|---|---|---|---|---|---|
| $f$ | $C_{fem}$ | $C_{est}$ | $C_{fem}$ | $C_{est}$ | $C_{fem}$ | $C_{est}$ | $C_{fem}$ | $C_{est}$ | $C_{fem}$ | $C_{est}$ | $C_{fem}$ | $C_{est}$ |
| **0.0** | 2.6266 | 2.6561 | 2.7439 | 2.8212 | 2.9404 | 3.0444 | 3.2477 | 3.3256 | 3.6158 | 3.6648 | 3.9577 | 4.0621 |
| **0.2** | 4.0284 | 3.9975 | 4.4010 | 4.2961 | 4.7046 | 4.6485 | 5.1593 | 5.0549 | 5.6721 | 5.5153 | 6.1233 | 6.0295 |
| **0.4** | 5.2001 | 5.0603 | 5.4741 | 5.4556 | 5.9983 | 5.9065 | 6.5304 | 6.4130 | 7.1121 | 6.9749 | 7.6256 | 7.5924 |
| **0.6** | 5.8437 | 5.8443 | 6.1406 | 6.2999 | 6.6468 | 6.8184 | 7.3934 | 7.3996 | 8.0380 | 8.0437 | 8.6193 | 8.7507 |
| **0.8** | 6.3350 | 6.3497 | 6.6486 | 6.8290 | 7.1938 | 7.3840 | 7.9801 | 8.0150 | 8.6818 | 8.7218 | 9.3243 | 9.5044 |
| **1.0** | 6.7031 | 6.7031 | 7.0285 | 7.0285 | 7.6054 | 7.6054 | 8.4310 | 8.4310 | 9.1804 | 9.1804 | 9.8695 | 9.8695 |

## 5. Algebraic Equations

From Table (3), one can observe that critical loads are increasing function of analysis parameters, $f$ and $\gamma$. Generally, the results obtained by numerical methods are effective only for the particular values of parameters considered in the analysis. In other words, numerical analysis results are valid only for the discrete parameters. In addition, the structural engineers may need concise formulas to make their design or stability checks easy.

With these points in mind, the changes of critical load coefficient is represented by algebraic function of parameters, $f$ and $\gamma$.

$$C_{est}= C_{fem}= (A_0+A_1 f+A_2 f^2) + (B_0+B_1 f+B_2 f^2)\gamma+(C_0+C_1 f+C_2 f^2)\gamma^2 \tag{14}$$

The numerical values of coefficients, $A_0, A_1, \cdots, C_2$ are determined by the regression technique. Again, because of space limits, only some results are listed in Table (4).

## Table (4). Regression constants

<Fig. 1(a), Fig. 2(a)>

| λ | A0 | A1 | A2 | B0 | B1 | B2 | C0 | C1 | C2 | ρ |
|---|---|---|---|---|---|---|---|---|---|---|
| 1.0 | 6.2918 | 12.2290 | -5.3350 | -0.8680 | 0.2898 | -0.6059 | -1.4681 | -1.7380 | 0.8764 | 0.9996 |
| 1.4 | 4.0276 | 7.2956 | -3.3701 | 2.1151 | 6.0608 | -3.1926 | -1.6427 | -6.5322 | 3.5846 | 0.9726 |
| 1.8 | 4.1598 | 7.6928 | -4.065 | 1.9552 | -3.5904 | 3.0226 | -2.0956 | 2.6641 | -1.7117 | 0.9945 |
| 2.2 | 4.1742 | 5.1023 | -1.9475 | 0.3190 | 4.1907 | -3.4174 | -0.1569 | -4.083 | 3.2438 | 0.9875 |
| 2.6 | 4.0335 | 5.9419 | -2.8781 | 1.1311 | -3.3703 | 3.0809 | -1.0610 | 2.9603 | -2.5104 | 0.9958 |
| 3.0 | 4.1456 | 4.6455 | -1.6760 | 0.3939 | 0.7513 | -0.7398 | -0.4939 | 0.0281 | 0.1675 | 0.9972 |

<Fig. 1(a), Fig. 2(b)>

| λ | A0 | A1 | A2 | B0 | B1 | B2 | C0 | C1 | C2 | ρ |
|---|---|---|---|---|---|---|---|---|---|---|
| 1.0 | 3.9010 | 5.3953 | -2.1821 | -0.8747 | 0.1964 | -1.2037 | -1.4211 | -0.3260 | 0.5450 | 0.9886 |
| 1.4 | 3.9595 | 1.4553 | -0.6701 | 1.8809 | -0.5802 | 0.1873 | -1.3391 | 1.4288 | -0.9777 | 0.9428 |
| 1.8 | 4.0103 | 0.2926 | -0.0987 | 2.3796 | -0.2269 | -0.4294 | -2.3937 | 2.5602 | -0.9799 | 0.9060 |
| 2.2 | 4.1327 | 0.5101 | -0.2216 | 0.2765 | 1.1024 | -0.9325 | -0.1445 | -1.0037 | 0.8765 | 0.9161 |
| 2.6 | 3.9010 | 0.4365 | -0.2413 | 1.2908 | -2.2866 | 1.5385 | -1.1114 | 3.3563 | -2.4314 | 0.9208 |
| 3.0 | 4.1322 | -0.0543 | 0.2371 | 0.3226 | 1.1464 | -1.3029 | -0.4673 | -0.1968 | 0.5178 | 0.9408 |

<Fig. 1(a), Fig. 2(c)>

| λ | A0 | A1 | A2 | B0 | B1 | B2 | C0 | C1 | C2 | ρ |
|---|---|---|---|---|---|---|---|---|---|---|
| 1.0 | 6.2168 | 8.3104 | -3.6910 | -0.9553 | 0.3942 | 3.8171 | -1.4387 | -1.8058 | -3.3793 | 1.0000 |
| 1.4 | 3.9879 | 7.0169 | -3.0745 | 2.2359 | 6.2390 | -3.5711 | -1.7658 | -10.5240 | 6.1564 | 0.9756 |
| 1.8 | 4.1796 | 6.7857 | -3.3225 | 1.7530 | -1.1903 | 2.4525 | -1.9574 | -0.0751 | -1.8416 | 0.9767 |
| 2.2 | 4.1398 | 5.3596 | -2.1321 | 0.4306 | 4.4050 | -3.5325 | -0.2660 | -6.5131 | 5.0027 | 0.9936 |
| 2.6 | 4.0334 | 5.5642 | -2.5002 | 0.9743 | -0.5801 | 0.3620 | -0.8940 | -0.9665 | 1.1504 | 0.9954 |
| 3.0 | 4.1315 | 4.5830 | -1.6198 | 0.4777 | 1.4823 | -1.2103 | -0.6184 | -1.1626 | 0.8305 | 0.9958 |

<Fig. 2(a), Fig. 2(a)>

| λ | A0 | A1 | A2 | B0 | B1 | B2 | C0 | C1 | C2 | ρ |
|---|---|---|---|---|---|---|---|---|---|---|
| 1.0 | 2.6361 | 7.4037 | -3.4833 | 0.6806 | 3.8801 | -2.4660 | 0.7254 | -0.4353 | 0.8923 | 0.9859 |
| 1.4 | 2.9698 | 5.4057 | -2.1848 | 0.5212 | 0.9684 | -0.4221 | 1.0114 | 0.3763 | -0.2613 | 0.9891 |
| 1.8 | 2.9130 | 6.3789 | -2.9522 | 0.6728 | 2.3908 | -1.8340 | 0.4849 | -1.7169 | 1.6373 | 0.9771 |
| 2.2 | 3.0337 | 5.7106 | -2.3142 | 0.4406 | 1.9976 | -1.3765 | 0.8773 | -2.4755 | 1.5661 | 0.9757 |
| 2.6 | 3.0037 | 6.1761 | -2.7990 | 0.8308 | 1.2520 | -1.0819 | 0.2775 | -1.7633 | 1.4418 | 0.9709 |
| 3.0 | 2.9759 | 6.7228 | -3.2005 | 1.2000 | -4.3551 | 4.2398 | 0.0361 | 1.1433 | -1.5158 | 0.8918 |

<Fig. 2(a), Fig. 2(b)>

| λ | A0 | A1 | A2 | B0 | B1 | B2 | C0 | C1 | C2 | ρ |
|---|---|---|---|---|---|---|---|---|---|---|
| 1.0 | 2.6473 | 4.3162 | -2.2719 | 0.5705 | 0.7833 | -0.4981 | 0.8084 | 0.1589 | 0.1133 | 0.9897 |
| 1.4 | 2.9700 | 3.4672 | -1.5588 | 0.4679 | 3.1182 | -2.3417 | 1.0730 | -4.0161 | 2.1623 | 0.9669 |
| 1.8 | 2.8099 | 3.4027 | -1.9045 | 0.6394 | -0.0028 | -0.1192 | 0.4552 | -0.1653 | -0.1146 | 0.9711 |
| 2.2 | 3.0656 | 3.5053 | -2.2444 | 0.4914 | 0.4725 | -0.6457 | 0.7312 | -3.4011 | 2.6321 | 0.9389 |
| 2.6 | 3.0139 | 3.1443 | -1.9038 | 0.7962 | -1.1906 | 0.8838 | 0.2659 | -0.4822 | -0.0320 | 0.9551 |
| 3.0 | 3.0181 | 3.1445 | -2.0087 | 0.8751 | -1.3191 | 0.6544 | 0.1225 | -0.9379 | 0.7908 | 0.9376 |

<Fig. 2(a), Fig. 2(c)>

| λ | A0 | A1 | A2 | B0 | B1 | B2 | C0 | C1 | C2 | ρ |
|---|---|---|---|---|---|---|---|---|---|---|
| 1.0 | 2.6583 | 3.3623 | -2.1129 | 0.6741 | 0.9672 | -1.2275 | 0.6159 | 2.6494 | -0.1119 | 1.0000 |
| 1.4 | 2.9657 | 1.4760 | -0.4522 | 0.5047 | 0.5484 | 0.1025 | 0.9928 | 1.0305 | -0.2949 | 1.0000 |
| 1.8 | 2.9199 | 2.4453 | -1.3081 | 0.6726 | 1.0071 | -0.3743 | 0.4510 | 1.8845 | -0.8328 | 1.0000 |
| 2.2 | 3.8316 | -1.0617 | 1.4252 | -0.0073 | 3.7194 | -2.2168 | 0.4741 | 0.8678 | -0.0597 | 0.9780 |
| 2.6 | 2.9778 | 2.1948 | -1.0559 | 0.9089 | -0.7224 | 1.2864 | 0.2369 | 2.6088 | -1.1741 | 0.9879 |
| 3.0 | 2.9898 | 2.0885 | -0.9813 | 0.8569 | 1.4674 | -0.6579 | 0.1640 | 1.3502 | -0.3308 | 1.0000 |

In Table (3), the columns, $C_{est}$s denote the critical load coefficients estimated by Eq. (14) and Table (4). The comparison of $C_{fem}$ and $C_{est}$ reveals insignificant differences in any case, which justifies the proposed algebraic equation, Eq. (14). Actually the correlation coefficient, $\rho$ between $C_{fem}$ and $C_{est}$ calculated by Eq. (15) is almost unity ( $\rho \fallingdotseq 1$) for any combination of loading and boundary conditions,

$$\rho = \frac{\sum(C_{fem} - \overline{C}_{fem}) \cdot (C_{est} - \overline{C}_{est})}{\sqrt{\sum(C_{fem} - \overline{C}_{fem})^2 \cdot \sum(C_{est} - \overline{C}_{est})^2}} \qquad (15)$$

$\overline{C}_{fem}$, $\overline{C}_{est}$ : mean values of $C_{fem}$ and $C_{est}$

which proves the validity of the proposed algebraic equation.

## 6. Conclusions

The stability analysis of rectangular plates under two different types of patch loading conditions was performed by the finite element method. The parameters considered in the numerical analysis are aspect ratio of the plate, patch load width factor and Kinney's partial fixity factor.

As expected, stability of the plate is increased when the restraints at the edges are increased. If possible, the application of patch loads around the edge corners are preferable to the patch load at the edge center. The critical load changes due to the aspect ratio changes are not significant when the plate's aspect ratio is larger than 1.4.

The algebraic equation expressed by analysis parameters predicts fairly well the critical load changes determined by the finite element method. The correlation coefficient between $C_{fem}$ (=critical load coefficient by FEM) and $C_{est}$ (=coefficient by the algebraic equation) is almost unity ( $\rho \fallingdotseq 1.0$) for any aspect ratio, which suggests the design aid role of proposed equation.

### 7. Reference


1. SHARP M.L., "Behavior of Plates under Partial Edge Loading" , Proceedings of the Sessions Related to Steel Structures, Structures Congress 89, San Francisco, 1989, pp.215-224.
2. KHAN M.Z., JOHNS K.C., "Buckling of Plate with Partially Loaded Edges" , J. Struct. Eng. Div. Proc. ASCE ST 3, 1977, PP.547-588.
3. WHITE N., COTTINGHAM W.S., "Stability of Plates under Partial Edge Loadings" , J. Eng. Mech. Div. Proc. ASCE EM 5, 1962, PP.67-86.
4. CHAJES A., "Principles of Structural Stability Theory", Prentice-Hall, Inc., Englewood Cliffs, NJ, 1987.
5. KINNEY J.S., "Indeterminate Structural Analysis" , Addison Wesley Publishing Co., Massachusetts, USA, 1957.
6. KIM S.C., "Stress Analysis of Semi-Rigid Frame" , Proceedings of COSEIK Fall Symposium., Seoul, Korea, 1998.
7. SPIEGEL M.R., "Probability and Statistics", McGraw-Hill Book Co., New York, 1975.
8. LEE S.G., KIM S.C., SONG J.G., "Critical Loads of Square Plates under Different In-Plane Load Configrations on Opposite Edges" , International Journal of Structural Stability and Dynamics, Vol. 1, No. 2, 2001, pp.283-291.